Contents lists available at ScienceDirect

Ceramics International

CrossMark

Calcium–magnesium aluminosilicate corrosion of barium–strontium aluminosilicates with different strontium content

Fengrui Jiang, Laifei Cheng, Yiguang Wang*, Xuanxuan Huang

Science and Technology on Thermostructural Composite Materials Laboratory, Northwestern Polytechnical University, Xi'an, Shaanxi 710072, PR China

ARTICLE INFO

ABSTRACT

In this study, the hot corrosion of barium–strontium aluminosilicate ($B_{1-x}S_xAS$) attacked by calcium–magnesium aluminosilicate (CMAS) was investigated at temperatures in the 1200–1400 °C range. Moreover, a corrosion mechanism based on the interdiffusion of Ba/Sr and Ca cations was also proposed. The proposed corrosion mechanism indicated the diffusion of Ba/Sr cations into the CMAS, and Ca cations into the $B_{1-x}S_xAS$ during the hot corrosion process. At 1200 °C, a thin corrosion zone was formed at the interface of $B_{1-x}S_xAS$ and CMAS due to weak diffusion of Ba/Sr and Ca cations. Further increase in the temperature led to an enhancement in the interdiffusion of Ba/Sr and Ca cations, thus significantly widening the corrosion zone. Moreover, oriental dendrites, identified as monoclinic $B_{1-x}S_xAS$, were found to precipitate in the molten CMAS. Attributed to the faster diffusion rate of Sr cations compared to that of the Ba cations, $B_{1-x}S_xAS$ with a higher Sr content was found to be more prone to CMAS-induced corrosion due to the rapid loss of Sr.

1. Introduction

In aircraft engines, components must withstand high temperatures and should have a long lifetime. These requirements are beyond the limits of traditional superalloys. Silicon carbide fiber-reinforced silicon carbide ceramic matrix (SiC_f/SiC) composites are widely considered as promising materials for application in the hot sections of aircraft engines due to their excellent properties, including low density, good mechanical properties at high temperatures, and high oxidation resistance in dry air [1–5]. However, SiC materials are susceptible to water vapor corrosion when exposed to the combustion gas due to the rapid removal of SiC via the formation of silicon hydrates, resulting in the eventual failure of the materials [6,7]. Therefore, various environmental barrier coatings (EBCs) have been developed to protect SiC_f/SiC components in combustion environments and improve their durability [8–11].

The combustion gas is a very complex mixture. Previous studies have mainly focused on the water vapor corrosion behavior [12–14] and hot corrosion behavior (mainly due to Na_2SO_4) [15–17] of EBC materials. Besides the aforementioned corrosive media, the combustion gas also contains foreign particles, such as sand, volcanic ash, and other siliceous particles, that are regularly sucked into the engine during operation [18,19]. At elevated temperatures, these ingested siliceous particulates are deposited on the surface of the protective EBCs, which leads to the formation of a molten glass film with a composition similar to calcium–magnesium aluminosilicate (CMAS). The molten glass can attack the coatings by forming low-viscosity materials or new phases, which alter the water vapor resistance or the oxygen/water vapor permeation, finally resulting in the degradation of the EBCs and the premature failure of the SiC_f/SiC composites underneath [20–23].

Barium–strontium aluminosilicate ($B_{1-x}S_xAS$, $0 \leq x \leq 1$) has been considered as an attractive EBC material for the protection of SiC_f/SiC composites because of its low Young's modulus, a coefficient of thermal expansion (CTE) similar to that of the SiC_f/SiC composites, and a very low silica activity [24]. It has been successfully applied in the hot sections of aircraft engines, and shows a good long-term durability in combustion environments at temperatures below 1300 °C. Several reports on the effect of CMAS on the hot corrosion behavior of $B_{1-x}S_xAS$ [25,26] indicated that the interaction between $B_{1-x}S_xAS$ and CMAS proceeded via a dissolution-reprecipitation mechanism, i.e., CMAS was considered to melt and dissolve the $B_{1-x}S_xAS$ through the grain boundaries, resulting in the recrystallization of $B_{1-x}S_xAS$ as a modified celsian phase. However, so far, the effect of the addition of strontium oxide (SrO) by substituting strontium (Sr) for barium (Ba) in $B_{1-x}S_xAS$ on the corrosion mechanism has not been studied in detail. Therefore, in this study, we investigated the effect of CMAS on the hot corrosion behavior of $B_{1-x}S_xAS$ samples with different Ba to Sr ratios at temperatures in the 1200–1400 °C range. The reactions between CMAS and $B_{1-x}S_xAS$ were systematically investigated, and a new

* Corresponding author.
  E-mail address: wangyiguang@nwpu.edu.cn (Y. Wang).

model for the corrosion mechanism was also proposed.

2. Experimental methods

The $B_{1-x}S_xAS$ ($x=0$, 0.25, 0.50, 0.75, and 1) powders were synthesized via the sol–gel method [27]. $BaCO_3$ (analytical grade, Zhongxin Fine Chemical Factory, Xi'an, China), $Sr(NO_3)_2$ (analytical grade, Bodi Chemical Corp., Tianjin, China), $Al(NO_3)_3\cdot 9H_2O$ (analytical grade, Hongyan Chemical Reagent Factory, Tianjin, China), and tetraethoxysilane (TEOS, analytical grade, Kemiou Chemical Reagent Corp., Tianjin, China) were used as raw materials and weighed according to the intended molar ratio of Ba:Sr:Al:Si=$1-x$:x:2:2 ($x=0$, 0.25, 0.5, 0.75, and 1). The materials were dissolved in a mixture of ethanol (4 parts) and aqueous citric acid (40 wt%) solution (1 part). Ammonia was then added to stabilize the pH at about 3–4. The solutions were stirred at room temperature until stable and transparent sols were obtained. Next, the sols were heated in an oven at 60 °C for 12 h and then at 120 °C for 24 h to prepare the $B_{1-x}S_xAS$ gels. These gels were annealed at 900 °C for 2 h, ball-milled for 20 h, and then freeze-dried to obtain fine powders. The powders were granulated and cold pressed at 200 MPa for 1 min into disks with a diameter of 13.5 mm and a thickness of 2 mm. Finally, the green disks were sintered at 1600 °C for 3 h in air to prepare dense $B_{1-x}S_xAS$ samples for the subsequent corrosion tests.

CMAS with a composition of 33Ca-9Mg-13Al-45Si (in mole percent of single cation oxide formula units) [28] was selected for this study. The CMAS disks were prepared by mixing reagent-grade fine powders of the individual oxides, i.e., calcium oxide, magnesium oxide, aluminum oxide, and silicon dioxide (all procured from Tianli Chemical Reagent Co., Ltd., Tianjin, China). The raw materials were weighed according to the intended molar ratio and then mixed for 24 h in a planetary ball mill (ND7-4L, Nanda Instrument Plant, Nanjing, China) with de-ionized water used as media. After drying, the powder mixtures were heated in air at 100 °C for 10 h and then at 1200 °C for 24 h. Following wet-milling and freeze-drying, the powders were granulated and cold pressed into disks with a diameter of 13.5 mm and a thickness of 1 mm. Finally, the green bodies were sintered in air at 1200 °C for 2 h to eventually prepare the dense CMAS samples.

The CMAS-induced corrosion of $B_{1-x}S_xAS$ was investigated using freestanding $B_{1-x}S_xAS$ disks. All $B_{1-x}S_xAS$ and CMAS disks were polished until a flat surface with ~1 µm finish was obtained. For each corrosion test, a CMAS disk was placed on top of a $B_{1-x}S_xAS$ disk with their polished surfaces facing each other. The samples were then placed in a zirconia crucible and annealed at 1200, 1300, or 1400 °C in air for 4 h. The phase compositions of the uncorroded and corroded $B_{1-x}S_xAS$ samples were analyzed by X-ray diffraction (XRD, D/max-2400, Rigaku, Tokyo, Japan) with Cu Kα radiation. The data were recorded in continuous scanning mode over the 2θ range from 10° to 70° at a scanning rate of 0.02°s^{-1}. Differential scanning calorimetry (DSC) measurements were performed over the temperature range from room temperature to 1400 °C using a simultaneous thermal analyzer (NETZSCH STA 449F3, Germany) to investigate the reactions between CMAS and $B_{1-x}S_xAS$. The heating rate was 5 °C min^{-1}. The onset and end temperatures of the peaks were determined by peak analyzer in Origin software, considering the drift of baseline. The cross-sections of the corroded samples were examined by scanning electron microscopy in backscattered electron mode (SEM-BSE, JEOL-6700F, Tokyo, Japan). The elemental compositions of the samples were obtained by energy-dispersive X-ray spectroscopy (EDS, EDAX, USA).

3. Results and discussion

3.1. Phase composition and differential scanning calorimetry analysis

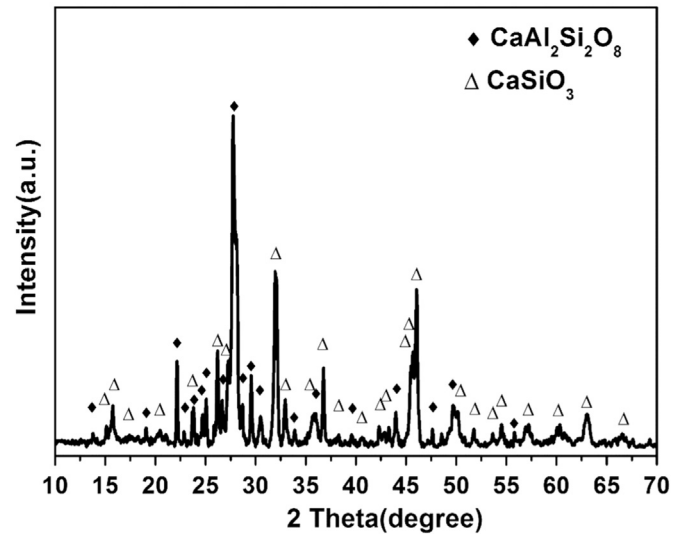The XRD pattern obtained for CMAS (Fig. 1) exhibits that the

Fig. 1. XRD pattern obtained for the CMAS sample after heat treatment at 1200 °C for 3 h.
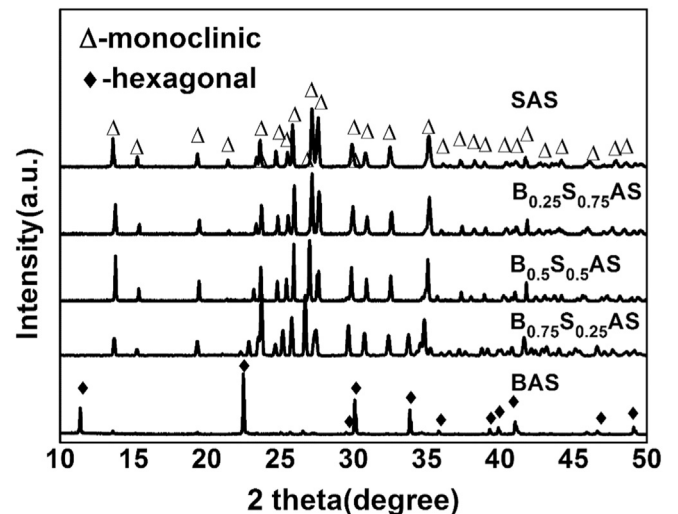

Fig. 2. XRD patterns obtained for the $B_{1-x}S_xAS$ ($x=0$, 0.25, 0.5, 0.75, and 1) samples after heat treatment at 1600 °C for 3 h.

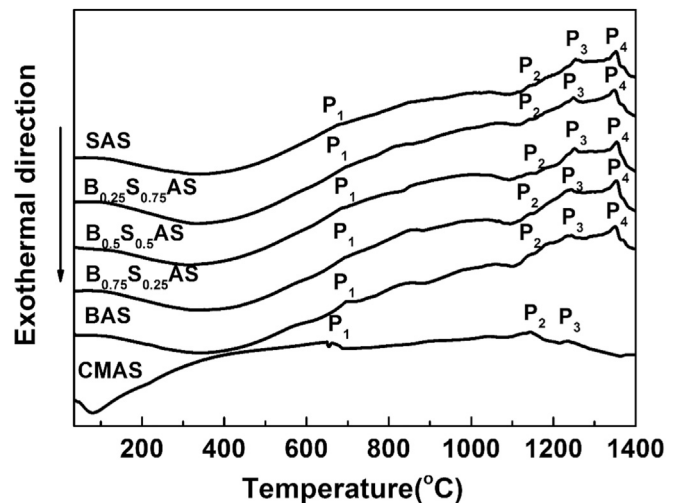**Fig. 3.** DSC patterns recorded for pure CMAS and the $B_{1-x}S_xAS$-CMAS systems ($x=0$, 0.25, 0.5, 0.75, and 1).